



## SEISMIC ISOLATION OF HIGH-RISE BUILDINGS USING THE FRICTION PENDULUM SYSTEM WITH FLUID VISCOUS DAMPERS

K. Zhong<sup>(1)</sup>, Y. Zhou<sup>(2)</sup>

<sup>(1)</sup>Graduate Student, Department of Civil and Environmental Engineering, Stanford University, kuanshi@stanford.edu

<sup>(2)</sup>Professor, State Key Laboratory of Disaster Reduction in Civil Engineering, Tongji University, yinzhou@tongji.edu.cn

### **Abstract**

In the past decade, the friction pendulum system (FPS) has been verified as a reliable seismic resisting. The longer vibration period and the concentration of energy dissipation are the underlying reasons for its effectiveness. However, its application in high-rise buildings is currently restrained by a major concern that the damage of superstructure is mitigated at the expense of excessive bearing deformations. In order to reduce the lateral displacement demand, one possible solution is to supply additional damping. This paper studies the seismic performance of the FPS supplemented by fluid viscous dampers. A design framework is proposed for this new seismic isolation system. Taking a high-rise shear-wall structure for example, the prototype design is also conducted to demonstrate this framework. Based on nonlinear time history analyses, it is found that fluid viscous dampers are able to control bearing deformations within the reasonable capacity. Bearing uplift, induced by the massive overturning moment, is considered in the proposed framework. By optimizing the layout of bearings, the uplift can be avoided in minor and moderate earthquakes. In major earthquakes, although slight uplifts are observed, the overall performance of the new seismic isolation system remains stable.

*Keywords: seismic isolation, friction pendulum system, fluid viscous damper, high-rise building, uplift*



## 1. Introduction

Severe lessons from recent earthquakes have triggered a rising consideration to protect and maintain tall buildings, one of the most vulnerable civil infrastructures. Ductility could protect the structure, but the considerable residual drift after a major earthquake will make the repair expensive and time-consuming [1]. In seismically-isolated structures, damages are mainly concentrated in the isolation story, which reduces the inelastic deformation in the superstructure. Comparing to the traditional seismic resisting systems, properly designed seismic isolation systems are able to improve the resilience of high-rise buildings.

The friction pendulum bearing (FPB) has its superiorities such as the high vertical load capacity, the large lateral deformation capacity, and the durability. There have been abundant works on its basic mechanical behavior as well as the modeling and design method for the friction pendulum system (FPS) [2-4].

In the past decade, the friction pendulum system (FPS) has been verified to be a reliable seismic resisting system for low-rise and middle-rise buildings. Theoretically, the FPS is effective for high-rise buildings; however, its application is currently shackled by two major concerns: (1) the excessive lateral bearing deformation [5, 6], and (2) the risk of bearing uplift due to increased overturning moments [7, 8].

The FPS supplemented by fluid viscous dampers in the isolation story is studied in this paper. Friction pendulum bearings undertake the vertical loads and mitigate seismic response of superstructure; while dampers assist in reducing bearing deformations and dissipating energy. Some previous researches have casted doubt on the additional damping. Based on the two-degree-of-freedom model, it has been proved that the linear damping could control the base vibration but also would diminish the isolation effect, i.e., increase the response of superstructure [9]. On the contrary, later researches stated based on time history analyses found that supplemental damping is favorable for isolation system [10]. This favorable effect was further verified by the systematical parameter analysis [11]. The analytical result also demonstrated that viscous damping is advantageous to the first mode of vibration but adverse to higher modes.

This paper will (1) investigate the new methodological framework for the design of the FPS supplemented by viscous dampers for high-rise buildings, and (2) conduct the prototype design of a 28-story shear-wall structure to demonstrate the proposed framework. Total 42 nonlinear time history analyses are conducted to study the seismic performance of the designed shear-wall structure. The isolation effect along with the force and displacement demands for bearings and dampers is checked to verify the design.

## 2. Methodological Framework

### 2.1 Performance objectives

The performance goals of building structures are concluded as the “two-stages-and-three-levels” method in the prevailing *Code for Seismic Design of Buildings (GB50011-2010)*. “Three levels” represent the minor, moderate, and major earthquake cases, with return periods of 50, 475, and 2475 years respectively. The correspondent performance goals are: (1) immediate occupancy without damage after minor earthquakes, (2) operational with repairable damage after moderate earthquakes, and (3) functional without severe collapse after major earthquakes. These objectives are achieved by checking forces and elastic displacements under minor earthquakes, and checking elastoplastic displacements under major earthquakes, which is so called “two stages”. Furthermore, the requirement for the moderate earthquake level is only satisfied by the design of structural detail [12].

### 2.2 Design framework

The seismic reduction ratio  $\beta$  is defined as the ratio of the peak response of the isolated building to the peak response of the fixed-base building under earthquakes. After Wenchuan earthquake, the current Chinese code for seismic isolation design has also revised the definition of seismic reduction ratio  $\beta$  for tall buildings ( $n$  stories): the maximum value of story shear ratios  $\beta_{V,i}$  and overturning moment ratios  $\beta_{M,i}$  under moderate earthquake



level (see Eq. (1) and Eq. (2), in which  $V_{i,isolated}$  and  $M_{i,isolated}$  are the story shear and overturning moment at the  $i^{th}$  story of the isolated structure, and  $V_{i,fixed}$  and  $M_{i,fixed}$  are the story shear and overturning moment at the  $i^{th}$  story of the fixed-base structure). Since the seismic reduction ratio  $\beta$  reflects the isolation effectiveness, it is used to determine the seismic reduction target (see Table 1).

In current Chinese seismic design code [12], Table 1 is adopted in design of seismic isolation system. For example, the structure is going to be built on the site having an original seismic intensity of 8 and a PGA of 0.30g, then the superstructure in the seismic isolation system can be designed using the seismic actions produced by the reduced intensity of 7 (0.15g) if the horizontal seismic reduction ratio (computed by Eq. 1 and 2) meets the corresponding limitation (for this case, it's 0.27~0.40) in Table 1.

$$\beta = \max \{ \beta_{V,1}, \beta_{V,2}, \dots, \beta_{V,n}, \beta_{M,1}, \beta_{M,2}, \dots, \beta_{M,n} \} \quad (1)$$

$$\begin{cases} \beta_{V,i} = \frac{V_{i,isolated}}{V_{i,fixed}} \\ \beta_{M,i} = \frac{M_{i,isolated}}{M_{i,fixed}} \end{cases} \quad i = 1, \dots, n \quad (2)$$

Table 1 - Relationship between the seismic reduction ratio and the reduced seismic intensity [12]

Original Seismic Intensity	Reduced Seismic Intensity		
	$0.53 \geq \beta \geq 0.40$	$0.40 > \beta > 0.27$	$\beta \leq 0.27$
9 (0.40g)	8 (0.30g)	8 (0.20g)	7 (0.15g)
8 (0.30g)	8 (0.20g)	7 (0.15g)	7 (0.10g)
8 (0.20g)	7 (0.15g)	7 (0.10g)	7 (0.10g)
7 (0.15g)	7 (0.10g)	7 (0.10g)	6 (0.05g)
7 (0.10g)	7 (0.10g)	6 (0.05g)	6 (0.05g)

Fig. 1 shows the design flowchart for the new seismic isolation system of high-rises. The preliminary design is based on the seismic reduction target for the superstructure. It consists of the superstructure design and the isolation system design. The design of superstructure could be conducted with a reduced seismic intensity if the design of the isolation system meets the required seismic reduction ratio. These two design stages will be respectively discussed in detail in the next two subsections.

### 2.3 Preliminary design stage

In preliminary design stage, there are four main tasks as follows: (1) to determine the layout of bearings, (2) to select the mechanical parameters of bearings, (3) to determine the layout of viscous dampers, and (4) to select the parameters of viscous dampers.

#### 2.3.1 Layout of bearings

In general, the interval distance between bearings is designed according to the vertical force capacity of the bearing. It is a common way to design bearings consistent with the column grid. However, in some case, the uplift could be mitigated by adjusting the location of some bearings. It might be a more practical and convenient approach comparing to using various restraint devices for bearings.

The bearing uplift is induced by the overturning moment. The overturning moment of the first story could be estimated by Eq. (3).



$$M_{ot} = \beta_{M,1} \sum_{i=1}^n F_{1i} h_i \leq \beta S_a(\zeta, T_1) \sum_{i=1}^n m_i h_i X_{1i} \frac{\sum_{k=1}^n m_k X_{1k}}{\sum_{k=1}^n m_k X_{1k}^2} \quad (3)$$

where  $\beta_{M,1}$  is the seismic reduction ratio based on the overturning moment of the first story, which is equal or less than  $\beta$ ;  $F_{1i}$  is the seismic action of the  $i^{th}$  particle in the simplified mass-spring model;  $X_{1k}$  is the first mode shape value of the  $k^{th}$  particle;  $S_a(\zeta, T_1)$  is the pseudo-acceleration of the first vibration mode.

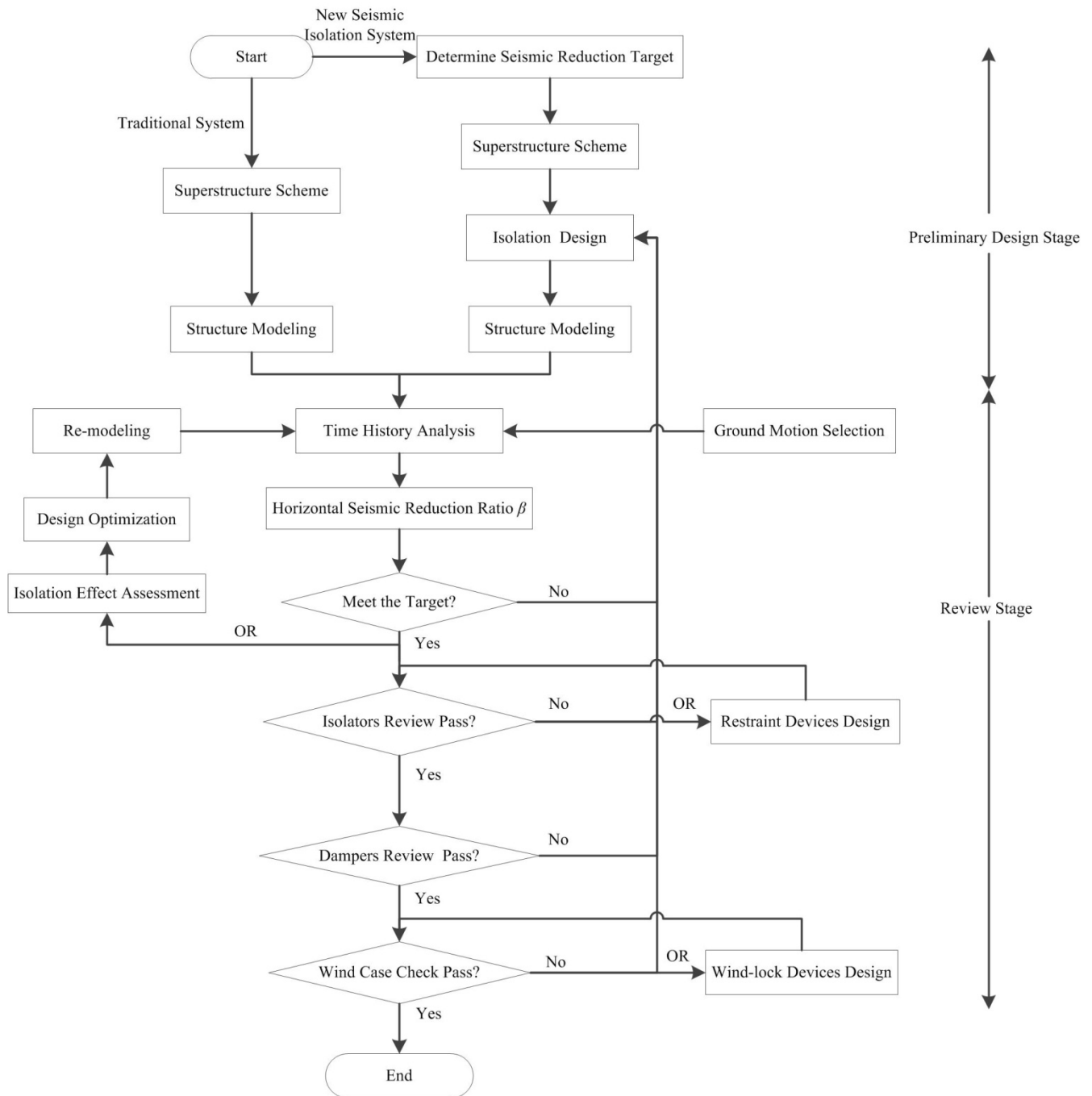


Fig. 1 –Flowchart for the new seismic isolation design of high-rise buildings

The moment equilibrium in the isolation story is shown in Eq. (4), where  $N_k$  is the vertical force



(compressive) of  $k^{th}$  bearing at  $y_k$  away from the neutral axis;  $t$  is the total number of bearings.  $N_k$  consists of two parts: the static gravity loading and the overturning-induced force.

$$M_{ot} = \sum_{k=1}^t N_k y_k = \sum_{k=1}^t \left( \frac{g \sum_{i=1}^n m_i}{t} + \lambda_1 y_k \right) y_k = \lambda_1 \sum_{k=1}^t y_k^2 \quad (4)$$

To avoid the uplift, the maximum overturning force  $N_{uplift,i}$  on the bearing should not exceed the vertical loading effect  $N_{s,i}$ :

$$N_{uplift} = \lambda_1 y_i \leq \frac{\beta S_a(\xi, T_1)}{\sum_{k=1}^t y_k^2} \Omega_1 y_i \leq N_{s,i} \quad (5)$$

$$\Omega_1 = \frac{\sum_{i=1}^n m_i h_i X_{1i} \frac{\sum_{k=1}^n m_k X_{1k}}{\sum_{k=1}^n m_k X_{1k}^2}}{\sum_{k=1}^n m_k X_{1k}^2} \quad (6)$$

Simplify Eq. (5), the criterion for avoiding the bearing uplift could be expressed in Eq. (7). There is no doubt that the bearings at corners are more vulnerable of uplift. Therefore, critical condition could be checked by Eq. (7) with  $y_i = y_{max}$  in the preliminary design stage.

$$\frac{y_i}{\sum_{k=1}^t y_k^2} \leq \frac{N_{s,i}}{\beta S_a(\xi, T_1) \Omega_1}, i = 1, 2, \dots, t \quad (7)$$

This criterion also indicates how to design the bearings to mitigate the overturning effect. Generally, the  $\Omega_1$  and  $S_a(\xi, T_1)$  are dependent on the design of superstructure and might be of little flexibility to change. In order to fulfill Eq. (7), there are two strategies: (1) optimizing the layout to reduce the left-hand side term; or (2) increasing the vertical pressure  $N_{s,i}$  on the bearings.

### 2.3.2 Parameters of bearings

Eq. (8) is the well-known force-deformation relation for the single-cave FPB, based on the definition that the positive direction of restoring force is opposite to the positive direction of deformation.

$$F = \frac{N}{R} u - \mu N \operatorname{sgn}(\dot{u}) \quad (8)$$

In Eq. (8), the effective radius of the concave  $R$ , as the key parameter, influences the fundamental period of the isolated structure. It can be selected by the following procedure.

Firstly, compute the effective pseudo-acceleration of the fixed-base structure as the weighted mean of  $S_a$  of the first three translation modes (see Eq. (9)). The weight is the corresponding modal contribution factors  $\lambda_i$ . Because the vibration of isolated structure is concentrated in the first mode ( $\lambda_i^* \rightarrow 0, i \neq 1$ ), the required pseudo-acceleration of the isolated structure can be estimated by Eq. (10).

$$S_a^{fixed,y} = \frac{\sum_{i=1}^3 S_a(\xi, T_i)_{fixed,y} \times \lambda_i}{\sum_{i=1}^3 \lambda_i} \quad (9)$$

$$S_a^{isolated} = \beta \times \max \{ S_a^{fixed,x}, S_a^{fixed,y} \} \quad (10)$$

Secondly, the required vibration period  $T_{isolated}$  could be back-calculated from the response spectra.



Finally, the effective radius of the concave  $R$  can be determined by Eq. (11).

$$R = g \times \left( \frac{T_{isolated}}{2\pi} \right)^2 \quad (11)$$

### 2.3.3 Layout of viscous dampers

Since the main function of viscous dampers is to control the bearings' deformation, it is reasonable to install dampers at the corners and along the perimeter of the building. A pair of orthogonal dampers connected at the same column is recommended in this study as an economical and efficient layout.

### 2.3.4 Parameters of viscous dampers

The overall damping force in this study is selected as 20~25 percent of the design base shear ( $F_{BS}$ , under moderate earthquakes) of the conventional structure in a certain direction (see Eq. (12)).

$$\sum_j F_{D,j} \leq 25\% \times F_{BS} \quad (12)$$

With the assumption of rigid slab, the mean damping force demand is:

$$F_{D,j} = \frac{\sum_j F_{D,j}}{n_D} \leq \frac{25\% \times F_{BS}}{n_D} \quad (13)$$

Using the force-velocity relationship in Eq. (14) for fluid viscous damper, key parameters (the damping factor  $C_j$  and the exponent factor  $\alpha_j$ ) could be selected for preliminary design.

$$F_{D,j} = C_j \dot{u}_j^{\alpha_j} \operatorname{sgn}(\dot{u}_j) \quad (14)$$

Previous researches have given suggestions for appropriate parameters of dampers to achieve an expected structural control [13, 14]. However, the maximum velocity of dampers in the new seismic isolation system would be much higher than that of dampers in the superstructure. It is estimated empirically that the upper limit of the velocity is 1000mm/s with the desirable range of 400~600mm/s under moderate earthquakes, and 600~800mm/s under major earthquakes

## 2.4 Review stage

Similar to the traditional design process, it is also an iterative procedure pursuing the optimal design. It is a trade-off between the isolation effect and the demand for bearings and dampers.

### 2.4.1 Seismic reduction ratio

After time history analyses, the dynamic responses under the moderate earthquake level is used to compute the seismic reduction ratio. If the computed ratio exceeds the required ratio, then the iterative design should be performed until fulfilling the target.

### 2.4.2 Seismic check of bearings and dampers

The seismic check of bearings includes (1) maximum deformations under major earthquakes (with bidirectional input); and (2) axial forces in three earthquake levels (if the uplift is severe under major earthquakes, than the overall behaviors of the whole FPS should be checked).

As for viscous dampers, the maximum deformations under major earthquakes (with single-directional inputs) are used to check the displacement capacities. The designed force capacity of each damper should be checked under the major earthquake level.

### 3. Prototype Design

#### 3.1 Basic information of the prototype

The proposed design framework is demonstrated by the design of a 28-story reinforced concrete shear-wall structure in Kashi, Xinjiang Province, China. The total structure height is 83.1m. Fig. 2 shows the typical floor plan (1<sup>st</sup> to 27<sup>th</sup> story), which has an overall dimension of 21.15m×27.80m. According to preliminary design, the total mass of the superstructure is about 1.67×10<sup>4</sup>t (950 kilograms per square meter). The building is located in the Category II site with a site characteristic period of 0.45s. According to the intensity 8 (0.3g) of the local region, the PGA is 110gal for minor earthquakes, 300gal for moderate earthquakes, and 510gal for major earthquakes. The local basic wind pressure is 0.55kN/m<sup>2</sup> with a return period of 50 years. The seismic reduction target is determined by the investor, who desires to reduce the seismic intensity by one degree, i.e., from 8 (0.3g) to 7 (0.15g).

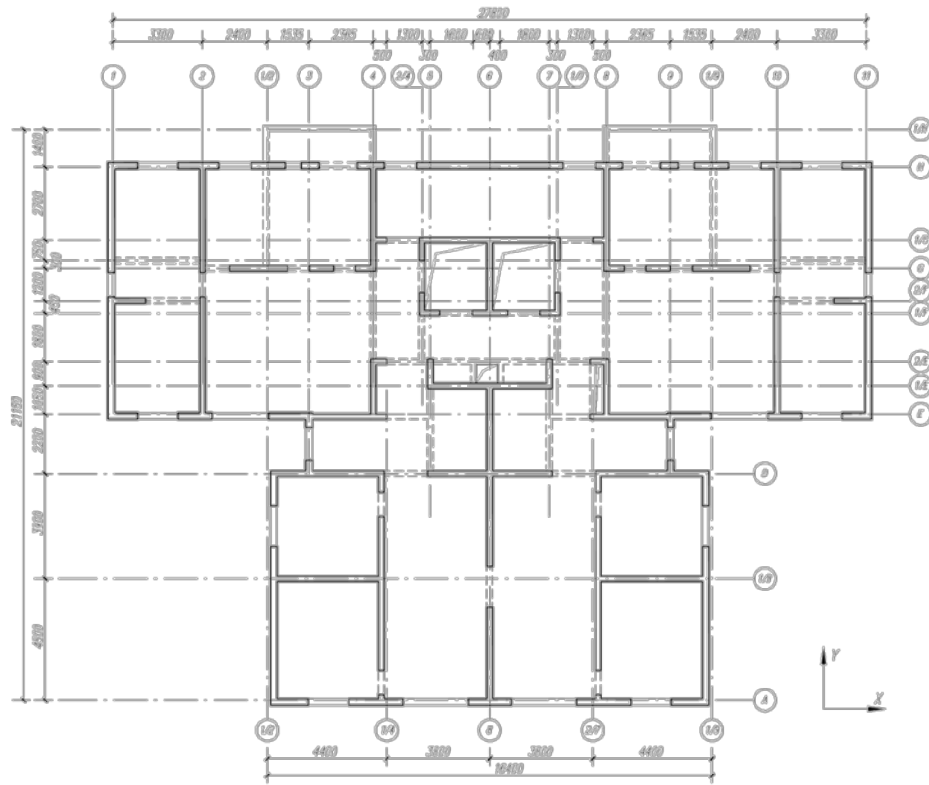


Fig. 2 – Plan view of the 1<sup>st</sup> to the 27<sup>th</sup> story

#### 3.2 Preliminary design

##### 3.2.1 Superstructure design

The design of isolated superstructure is of the same process as the traditional design of a fixed-base structure except for using the reduced seismic intensity. Table 2 shows the main parameters. The same design was applied in the fixed-base structure.

Table 2 - Selected design parameters for superstructure members

Story	Isolation Story	1 <sup>st</sup> -14 <sup>th</sup>	15 <sup>th</sup> -27 <sup>th</sup>	28 <sup>th</sup>
Concrete	C50	C40	C30	C30
Slab Thickness	160mm	120mm	120mm	120mm
Shear-wall Thickness	N/A	200mm, 250mm	200mm, 250mm	200mm, 250mm
Beam Cross-section	500mm×800mm	200mm×400mm	200mm×400mm	200mm×400mm
Column Cross-section	1200mm×1200mm	N/A	N/A	N/A

### 3.2.2 Seismic isolation system design

57 single-concave friction pendulum bearings are placed on the basement of the isolated structure. Table 3 lists the key parameters for the friction pendulum system. The overall size is the diameter of the bearing. Fig. 3 shows the bearing layout after the optimization to avoid the uplift under minor and moderate earthquakes.

Table 3 - Design parameters for friction pendulum system

Effective Radius $R$	Friction Coefficient $\mu$	Deformation before Sliding $u_y$	Maximum Eccentricity	Overall Size
5m	0.02	0.004m	0.20% in $y$ direction	1.2m

The base shear of the fixed structure under moderate earthquakes of Intensity 8 (0.3g) is about 40000kN in both main directions. According to Eq. (12) ~ Eq. (14), the total damping force demand is about 4000kN. 20 dampers are applied (10 in  $x$  direction, 10 in  $y$  direction), with  $C_{D,x}=C_{D,y}=400\text{kN}/(\text{m/s})^{0.2}$  and  $\alpha_x=\alpha_y=0.2$ . The deformation capacity of dampers is 500mm. The layout of FVD is shown in Fig. 3.

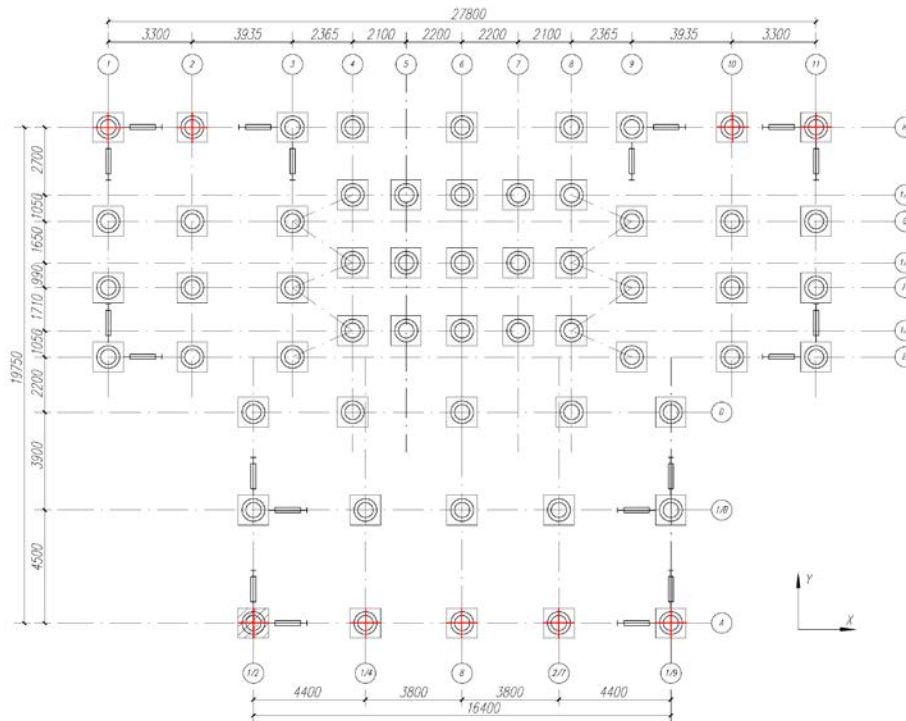


Fig. 3 – Plan view of the isolation story

Table 4 – Natural vibration periods

Mode	Period of the fixed-base structure (sec)	Period of the isolated structure(sec)
1 (translation in $y$ direction)	1.1448	4.6075
2 (translation in $x$ direction)	1.0184	4.5819
3 (rotation around $z$ axis)	0.6047	0.7960



### 3.2 Review stage

#### 3.2.1 Selection of ground motions

Five strong ground motion records were selected from the database of PEER-NGA Records. The two artificial ground motions were generated by SIMQKE\_GR code. The basic information of these seven records is listed in the Table 5. The mean spectrum and the target spectrum is plotted in Fig. 4. All the records were selected to match the target spectrum given by *Code for Seismic Design of Buildings (GB50011-2010)* for the minor earthquake level (Intensity 8, PGA=110gal), and scaled to the moderate earthquake level (PGA=300gal) and the major earthquake level (PGA=510gal) in the NLTHA.

Table 5 - Basic Information of Selected Ground Motions

Series	Year	Name	Station	Effective duration
NGA0075	1971	San Fernando	Maricopa Array #2	27.32s
NGA0800	1989	Loma Prieta	Salinas - John & Work	33.70s
NGA1291	1999	Chi-Chi, Taiwan	HWA044	60.50s
NGA1767	1999	Hector Mine	Banning - Twin Pines Road	40.88s
NGA2108	2002	Denali, Alaska	Eagle River - AK Geologic Mat	49.72s
AGM1	N/A	Artificial Ground Motion 1	N/A	33.93s
AGM2	N/A	Artificial Ground Motion 2	N/A	44.86s

Note: the effective duration denotes the bracketed duration in which ordinates are at least 10% of the amplitude.

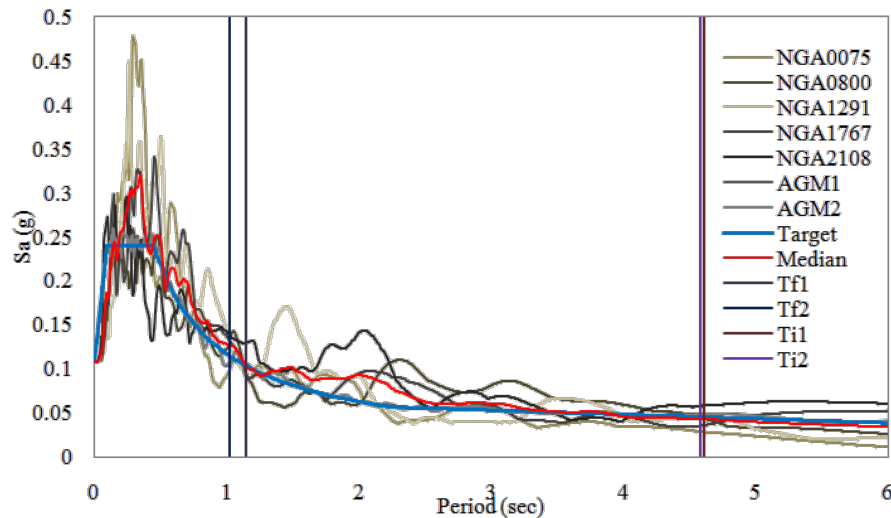


Fig. 4 – Pseudo-acceleration response spectra

#### 3.2.2 Seismic reduction ratio

Total 42 sets of nonlinear time history analyses at 3 hazard levels were conducted in ETABS. Based on the story shears and overturning moments under the moderate earthquake level (PGA=300gal), the seismic reduction ratios for each story in both directions were computed and plotted in the Fig. 5. The maximum ratio is 0.32 for the story shear in y direction, which matches the seismic reduction ratio target (0.27~0.40).

Fig. 6 shows the mean inter-story drift ratios under moderate earthquakes. As expected, the drift ratios were reduced by the new seismic isolation system. Comparing to elastic drift ratio of 0.001, it could be expected that severe nonlinear behavior occurred in the fixed-base structure, while the superstructure still maintained elastic in the isolated structure.

#### 3.2.3 Performance of bearings and dampers



Table 6 lists the maximum deformation of bearings (and connected dampers) under major earthquakes. The mean bearing displacements in both the two directions are under less than 0.5m. Table 7 lists the maximum damping forces of a single damper, the mean of which is also within the capacity of the devices.

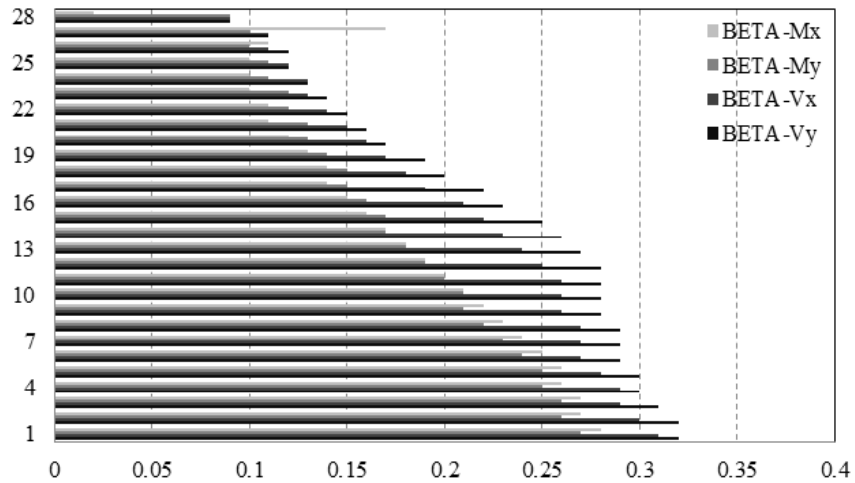


Fig. 5 -Seismic reduction ratio for each story

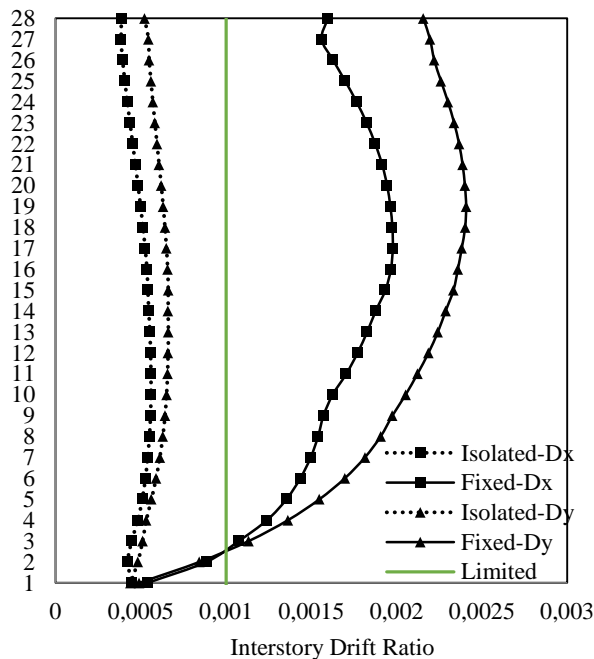


Fig. 6 – Mean inter-story drift ratio under moderate earthquakes (PGA=510gal)

Table 6 - Maximum deformation of bearings under major earthquakes (m)

NGA0075X	NGA0800X	NGA1291X	NGA1767X	NGA2108X	AGM1X	AMG2X	Mean X
0.2873	0.3899	0.3539	0.5937	0.7394	0.3655	0.3330	<b>0.4375</b>
NGA0075Y	NGA0800Y	NGA1291Y	NGA1767Y	NGA2108Y	AGM1Y	AMG2Y	Mean Y
0.2627	0.3726	0.3571	0.5876	0.7325	0.3520	0.3187	<b>0.4262</b>

Table 7 - Maximum damping force of a single FVD under major earthquakes (kN)

NGA0075X	NGA0800X	NGA1291X	NGA1767X	NGA2108X	AGM1X	AMG2X	Mean X
372.62	382.04	386.96	379.36	400.13	367.22	355.10	<b>377.63</b>
NGA0075Y	NGA0800Y	NGA1291Y	NGA1767Y	NGA2108Y	AGM1Y	AMG2Y	Mean Y
383.15	377.19	382.22	377.48	390.41	362.07	353.38	<b>375.13</b>

The mean of minimum axial force of each bearing under seven ground motions were checked. As a result, no uplift was observed under minor or moderate earthquake level after optimizing the bearing layout. However, nine corner bearings were slightly uplifted under high-level excitations.

Fig. 7 shows the cyclic behavior of one of uplifted bearings (the shadowed bearing in the Fig. 3) under NGA2108. It is indicated that under minor earthquakes, the seismic action was sufficient to overcome the friction coefficient of the sliding surface, and to trigger a stable hysteretic property. Under moderate earthquakes, the force-deformation loop had some fluctuations. Under major earthquakes, the hysteretic loop extremely shriveled on the positive displacement excursion.

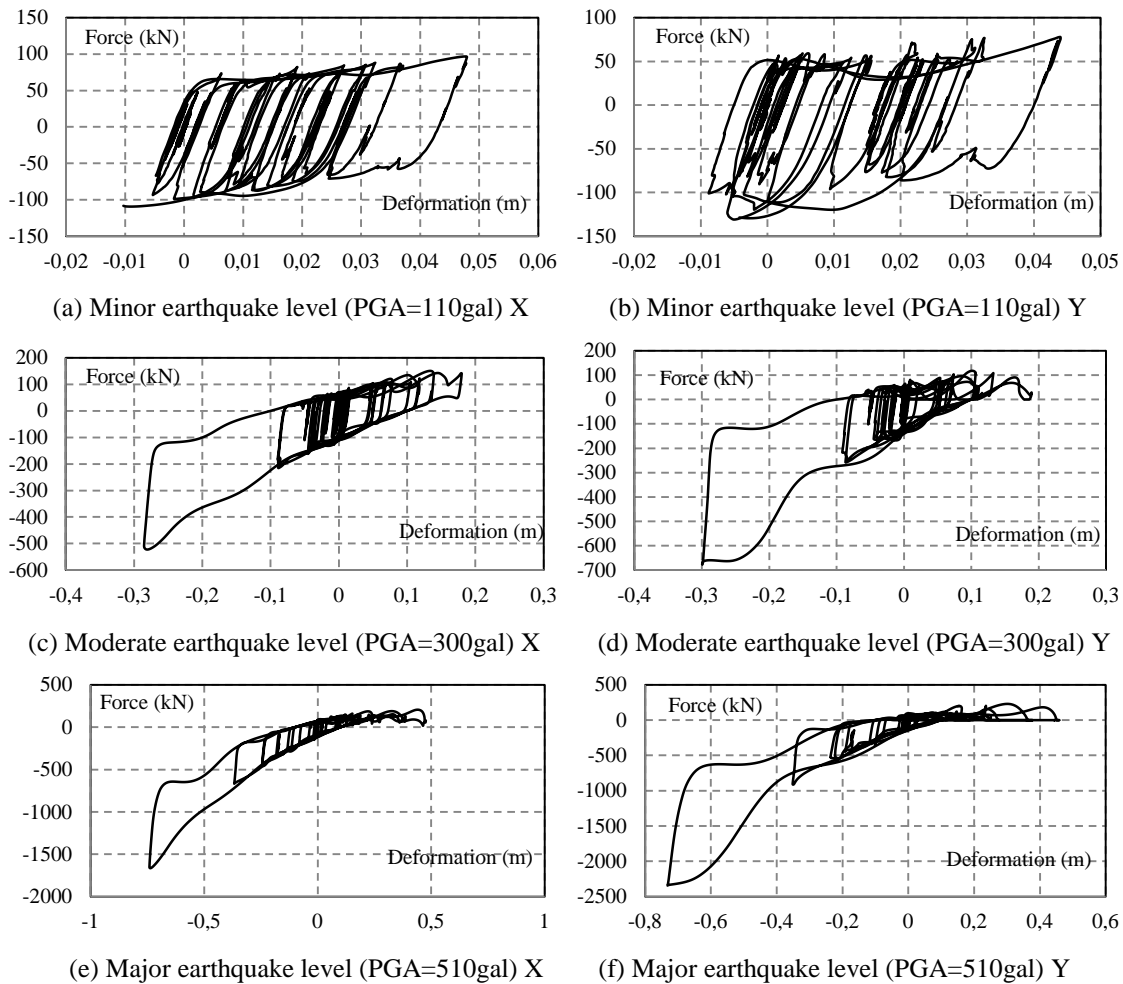
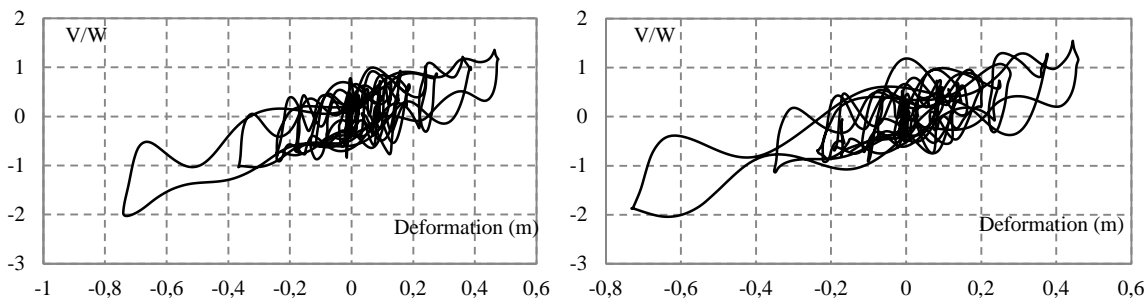


Fig. 7 - Cyclic behavior for the uplifted bearing

Fig. 8 shows the cyclic behavior of the overall friction pendulum system (57 bearings) under NGA2108. The total shear has been normalized with respect of the weight. It is found that the isolation system had a fairly stable behavior to protect the superstructure even under major earthquakes.





(a) Major earthquake level (PGA=510gal) X

(b) Major earthquake level (PGA=510gal) Y

Fig. 8 - Cyclic behavior for overall friction pendulum system

#### 4. Conclusions and Discussions

In this paper, the design framework for the new seismic isolation system of tall buildings is proposed. In the preliminary stage, mechanical parameters of the isolation system are determined, and the bearing layout is optimized to alleviate the potential uplift. The horizontal seismic reduction ratio and seismic performance of bearings and dampers are checked in the review stage. The prototypical design is conducted to demonstrate the proposed framework. Based on nonlinear time history analyses, it is found that supplemental dampers could reduce the bearing deformation demands to an acceptable level.

By optimizing the layout of bearings, the uplift can be avoided in minor and moderate earthquakes. In major earthquakes, although slight uplifts are observed, the overall performance of the new seismic isolation system remains stable. With the expectation to improve the reliability of seismic isolation in tall buildings, more uplift-proof or uplift-restraint strategies need to be studied in the future.

#### 5. Acknowledgements

The authors are grateful for financial support received from the National Natural Science Foundation of China (Grant No. 51322803) and Shu Guang project supported by Shanghai Municipal Education Commission and Shanghai Education Development Foundation (Grant No. 14SG19).

#### 6. References

- [1] Ramirez CM, Miranda E (2012): Significance of residual drifts in building earthquake loss estimation. *Earthquake Engineering & Structural Dynamics*, 41(11), 1477-1493.
- [2] Constantinou MC, Tadjbakhsh IG (1984): The optimum design of a base isolation system with frictional elements. *Earthquake engineering & structural dynamics*, 12(2), 203-214.
- [3] Zayas V, Low S, Mahin SA (1987): The FPS earthquake resisting system: experimental report. *UCB/EERC-87/01*, EERC, University of California, Berkeley, USA.
- [4] Mokha A, Constantinou MC, Reinhorn AM, Zayas VA (1991): Experimental study of friction-pendulum isolation system. *Journal of Structural Engineering*, 117(4), 1201-1217.
- [5] Nagarajaiah S, Sun X (2001): Base-isolated FCC building: impact response in Northridge earthquake. *Journal of Structural Engineering*, 127(9), 1063-1075.
- [6] Masroor A, Mosqueda G (2012): Experimental simulation of base-isolated buildings pounding against moat wall and effects on superstructure response. *Earthquake Engineering & Structural Dynamics*, 41(14), 2093-2109.
- [7] Koh AS, Hsiung CM (1991): Base isolation benefits of 3-D rocking and uplift. I: Theory. *Journal of engineering mechanics*, 117(1), 1-18.
- [8] Ryan KL, Chopra AK (2006): Estimating seismic demands for isolation bearings with building overturning effects. *Journal of Structural Engineering*, 132(7), 1118-1128.
- [9] Kelly JM (1999): The role of damping in seismic isolation. *Earthquake engineering & structural dynamics*, 28(1), 3-20.
- [10] Hall JF, Ryan KL (2000): Isolated buildings and the 1997 UBC near-source factors. *Earthquake Spectra*, 16(2), 393-411.
- [11] Politopoulos I (2008): A review of adverse effects of damping in seismic isolation. *Earthquake Engineering & Structural Dynamics*, 37(3), 447-465.
- [12] MOHURD (Ministry of Housing and Urban-Rural Development of the People's Republic of China) (2010): *Code for Seismic Design of Buildings*. GB50011-2010, China Architecture and Building Press, Beijing. (in Chinese).
- [13] Gluck N, Reinhorn AM, Gluck J, Levy R (1996): Design of supplemental dampers for control of structures. *Journal of structural Engineering*, 122(12), 1394-1399.



- [14] Zhou Y, Lu X, Weng D, Zhang, R (2012): A practical design method for reinforced concrete structures with viscous dampers. *Engineering structures*, 39, 187-198.